Using Mode Shapes from Cell Phone Videos for Machinery Health Monitoring

Shawn Richardson, Mark Richardson
Vibrant Technology, Inc., Centennial, CO

Click here for the IMAC Power Point presentation.

ABSTRACT

A cell phone video offers a low-cost non-contacting alternative to traditional accelerometer-based methods for monitoring the health of plant operating equipment. The frequency bandwidth and video enhancement technology in modern-day cell phones have rendered them ideal for use as a non-contacting measurement device in a plantwide route-based monitoring program.

During the past 30 years, trained neural networks have been used in a variety of applications to solve problems where the number of possible solutions is overwhelming. A neural network must be trained with lots of data, and it will diagnose mechanical faults in rotating machinery more accurately as it is trained with more vibration data

In this paper, it is first shown how the Operational Modal Analysis (**OMA**) mode shapes of a rotating machine are obtained by using **FRF-based** curve fitting on vibration data extracted from a cell phone video recording of a rotating machine during operation. Then, a database search method called **FaCTs™** is used to identify various unbalance conditions of the rotating machine.

FaCTs™ functions in the same manner as a trained neural network. **FaCTs™** uses the current mode shapes of a machine together with a shape difference indicator (**SDI**) to find the ***closest match*** of the current mode shapes with mode shapes that were previously ***labeled*** and ***archived*** in a database. **FaCTs™** displays a bar chart of the ***ten closest matches*** of the current mode shapes with the labeled mode shapes, thereby indentifying the current mechanical condition of a machine based on its mode shapes.

KEY WORDS

Artificial Intelligence (**AI**), Neural Network (**NN**), Time Waveform (**TWF**), Digital Fourier Transform (**DFT**), Operational Modal Analysis (**OMA**) mode shape, Operating Deflection Shape (**ODS**), Degree of Freedom (**DOF**), Frames Per Second (**fps**), Auto Power Spectrum (**APS**), Cross Power Spectrum (**XPS**), **ODS-FRF** (**APS** & **Phase** of an **XPS** with a reference), Fault Correlation Tools (**FaCTs™**), Shape Difference Indicator (**SDI**)

ROTATING MACHINE

In this paper, **FaCTs™** is used to uniquely identify ***nine different unbalance cases*** of the rotating machine shown in Figure 1. The machine has a variable speed motor connected to the rotor with a rubber belt. The motor speed was adjusted so that the rotor speed was ***approximately 1000 RPM throughout all the video recordings***.

Figure 1. Rotating Machine Showing Unbalance Screws Added to Its Rotors

INTRODUCTION

Most power plants, oil refineries, and manufacturing plants worldwide have implemented route-based machinery health monitoring programs for accessing the health of their rotating equipment. Digital vibration signals are the primary data used to detect and diagnose faults in operating equipment.

Traditionally, machine health monitoring has been done by attaching accelerometers to the surfaces of the operating equipment and acquiring vibration signals from the accelerometers using a portable digital spectrum analyzer. This method of data acquisition is time consuming and expensive compared with a cell phone video recording. Furthermore, because it is non-contacting, a cell phone can record vibration of machine parts that are too hot or inaccessible for attaching accelerometers.

In previous papers [3], [4] we applied traditional signal processing methods to the **TWFs** extracted from the frames of a video to display its **ODS's** in animation. **Time-based ODS's** can be displayed by sweeping a cursor through the **TWFs**, and **frequency-based ODS's** can be displayed using sinusoidal modulation of the ODS at a cursor position in the **DFTs**. Deformations can be displayed at ***slower speeds*** with ***higher amplitudes*** to make machine vibration easier to visualize and understand.

In a previous paper [4], a new database search method called **FaCTs™** was introduced, and was used to uniquely identify nine different unbalance cases of a rotating machine using only **ODS** data from the tops of the two bearing blocks on the machine. In this paper **FaCTs™** is used to uniquely identify the same nine unbalance cases using the **OMA** mode shapes of the machine.

These results demonstrate the reliability and repeatability of **OMA** mode shapes extracted from cell phone videos for machine health monitoring. **FaCTs™** also functions like a neural network in that it becomes more accurate as more ***labeled*** and ***archived*** **OMA** mode shapes are added to an archival database.

ARTIFICIAL INTELLIGENCE (OR MACHINE LEARNING)

Artificial Intelligence, popularly known as **AI**, uses a ***trained*** neural network (**NN**) to infer the meaning of a set of data. For example, the trained inference software in a Tesla car uses data from eight digital cameras to control the car.

Vibration data is primarily used to diagnose the health of rotating machinery. Vibration data in the form of **TWFs**, **DFTs**, **ODS-FRFs**, **ODS's** and **Mode Shapes** can be used to train an **NN**. But to accurately diagnose a mechanical fault, an **NN** ***must be trained with a lot of vibration data***.

Here are a couple definitions of **AI** from a Google search on the Internet.

- A neural network is a machine learning model that uses a network of interconnected nodes, or artificial neurons, to process data in a way that mimics the human brain.
- A neural network is a method in artificial intelligence (**AI**) that teaches computers to process data in a way that is inspired by the human brain. It is a type of machine learning (**ML**) process, called deep learning, that uses interconnected nodes or neurons in a layered structure that resembles the human brain. Machine Learning (**ML**) using an **NN** mimics the learning of the human brain. An **NN** is depicted in Figure 2

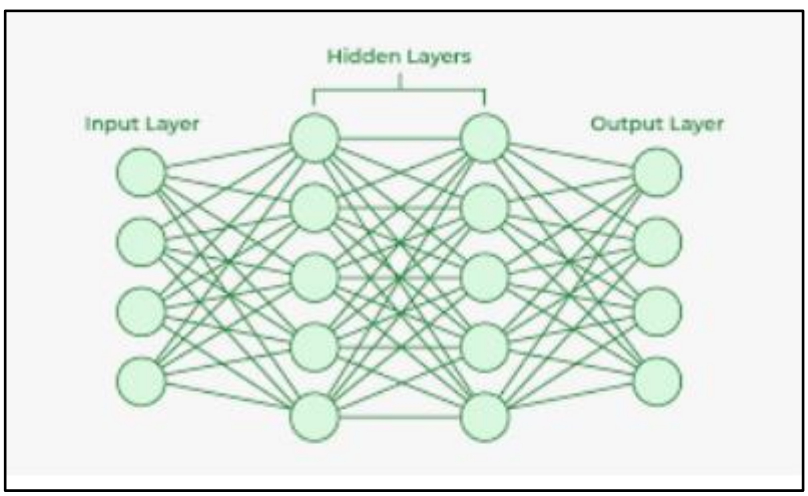

Figure 2. A Neural Network

- ***Lots of labeled input data*** is required to train an **NN**
- To diagnose mechanical faults, an **NN** must be trained with data that is ***uniquely associated with a mechanical fault***
- When vibration data is input to an Inference Engine (a trained **NN**), it diagnoses a mechanical fault, as shown in Figure 3.

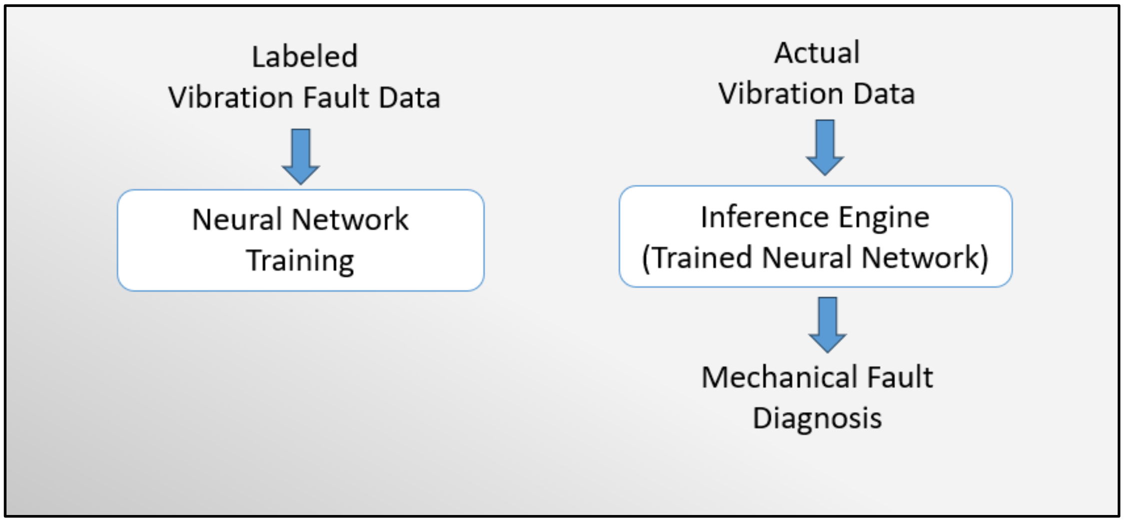

Figure 3. NN Training & Inference Engine

TWFs & DFTs

When a video is processed in MEscope [8], a rectangular grid of points with rectangular surfaces between them is created. Frames of the video are attached to this surface during animated display of **ODS's** extracted from the video. Using a rectangular point grid, ***millions of pixels*** in each frame of a cell phone video are processed to extract **TWFs** for the horizontal & vertical motion of ***thousands of points*** in the point grid. Grid points with ***little or no motion***, (like background points), are hidden and their linked **TWFs** are removed from further analysis. A point grid with background points hidden is shown in Figure 4.

A **DFT** is calculated for each **TWF** that is extracted from the video. Time-based **ODS's** are displayed in animation from the **TWFs** using a sweeping Line cursor. Frequency-based **ODS's** are displayed in animation from the **DFTs** using sine dwell modulation of the **ODS** at the cursor position. The **magnitude & phase** of the **ODS** at selected points can also be displayed, as illustrated in Figure 4.

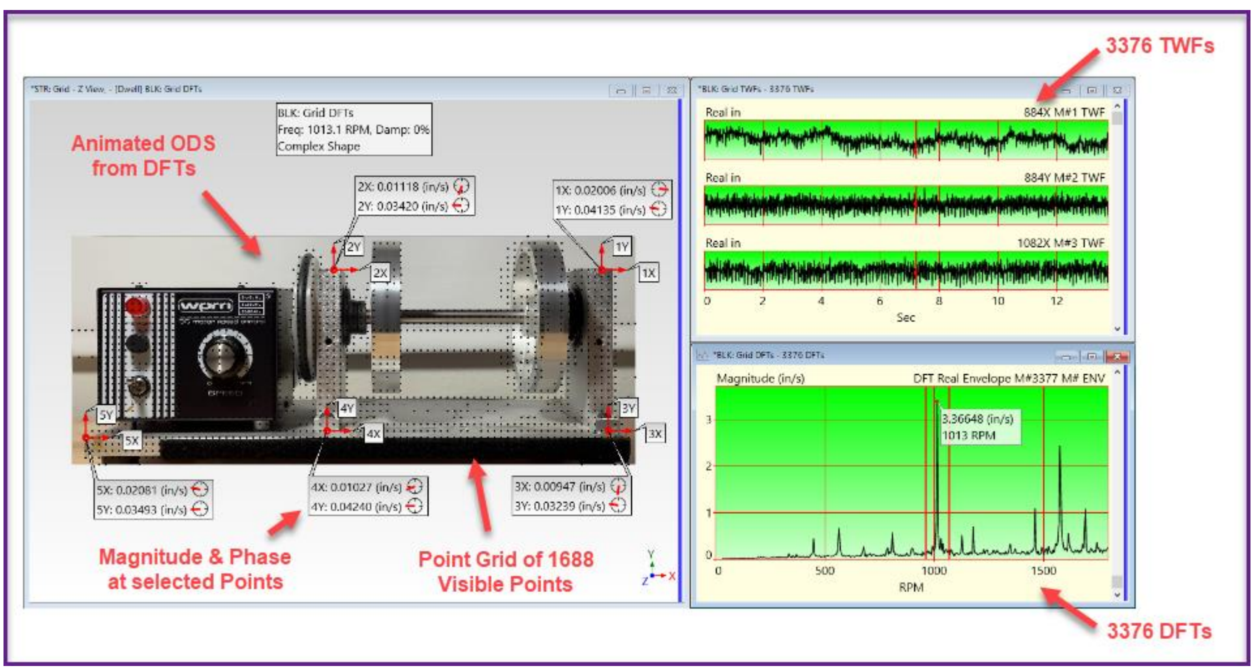

Figure 4. First-Order ODS Animated from DFTs

ODS-FRFs

A unique frequency domain function, called an **ODS-FRF,** can be calculated from each response **TWF** extracted from a video. A set of **ODS-FRFs** calculated from the **TWFs** is typically more accurate because ***spectrum averaging*** can be used to reduce extraneous noise from the **ODS-FRFs**.

The ***magnitude*** of an **ODS-FRF** is the **APS** of the ***response*** **DOF** at a grid point. The ***phase*** of the **ODS-FRF** is the ***phase of the*** **XPS** between the ***response*** **DOF** and the **DOF** of any ***reference*** grid point.

ODS-FRFs carry the ***same displacement units*** as the response **TWFs** from which they are calculated. But because it is a frequency domain function, an **ODS-FRF** can be ***accurately differentiated to velocity units*** by multiplying it by the frequency variable.

Vibration in ***velocity units*** is commonly used by vibration analysts to quantify vibration levels in rotating equipment.

LAW OF THE FFT

One of the laws of the **FFT** algorithm is that **Δf** = **1/T**, where **Δf** is the ***frequency difference between samples*** of an **ODS-FRF**, and **T** is the ***time length*** of **TWF** data from which the **ODS-FRF** was calculated. For example, if an **ODS-FRF** is calculated from **TWF** data over a **15 second** period, the frequency resolution (**Δf**) of the **ODS-FRF** is **60/15 = 4 RPM**.

To increase the frequency resolution of an **ODS-FRF**, **TWF** data over a ***longer period*** **T** is required. Therefore, the video from which the **TWFs** are extracted must be recorded over a ***longer period*** **T**.

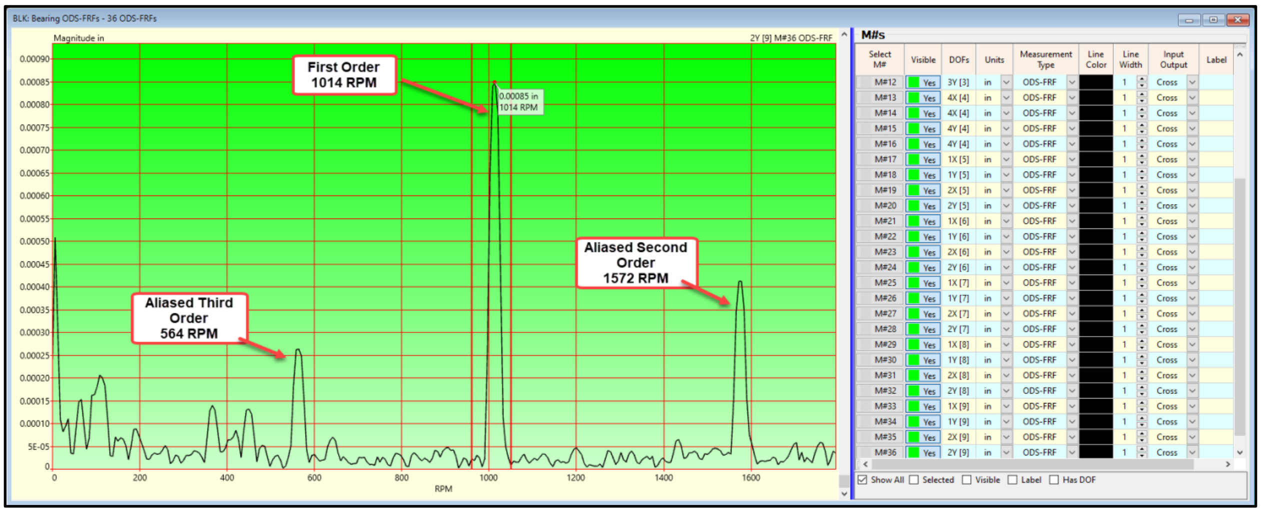

Figure 5. ODS-FRF Showing First Three Order Peaks.

ALIASED ORDER PEAKS

A limitation of any video recording is that ***anti-alias filtering cannot be used*** to remove high-frequency signals from the video.

Without anti-alias filtering, machine order peaks ***greater than one-half the sampling frequency***, (called **Fmax)**, are ***folded around*** **Fmax** and appear at lower frequencies in the **ODS-FRFs**, as shown in Figure 5.

All order-related resonance peaks between **Fmax & 2x Fmax** are folded around (***wrapped around***) **Fmax** and appear at a lower frequency in the frequency band **(0 to Fmax).** Aliasing of higher frequencies occurs in both **DFTs** and **ODS-FRFs**.

The **ODS-FRF** shown in Figure 5 was calculated from a **TWF** that was extracted from a video that was sampled at **60 fps**, or **3600 RPM**. Therefore, the **Fmax** of the **ODS-FRF** is **1800 RPM**. The first-order peak is at the machine running speed and is clearly visible at **1014 RPM**. The second order resonance peak should be at **2028 RPM** and third order resonance peak should be at **3042 RPM,** but they are ***folded around*** **1800 RPM** and both peaks are clearly visible ***at lower frequencies*** in the **ODS-FRF**.

The aliased frequency of any aliased order between **Fmax & 2x Fmax** can be calculated using a simple formula.

- **Second order** aliased frequency ➔ 1800 - (2028 - 1800) ➔ **1572 RPM**
- **Third order** aliased frequency ➔ 1800 - (3042 - 1800) ➔ **558 RPM**

The **ODS-FRF** in Figure 5 was calculated from a **TWF** with ***a 10-second length*** **T**. Therefore **Δf = (1/10) Hz or 60/10 = 6 RPM**. So, the aliased frequency of the third order peak ***is within one*** **(Δf)** of its calculated value.

CURVE FITTING THE ODS-FRFS

ODS-FRFs can be curve fit using an **FRF-based** curve fitter if they have been previously filtered using a special window. In MEscope [9] this filter is called a **DeConvolution window**. This filter reshapes an **ODS-FRF** so that it closely resembles an **FRF** and therefore can be curve fit using **FRF-based** curve fitting. An **FRF-based** curve fit of the three order peaks in an **ODS-FRF** is shown in Figure 6. In the upper left-hand graph, the **red curve fitting function** is overlaid on a magnitude plot of the **ODS-FRF**.

The aliased frequencies of the second and third orders are correctly estimated by curve fitting the **ODS-FRF**. More details on curve fitting **ODS-FRFs** are given in a companion paper [1].

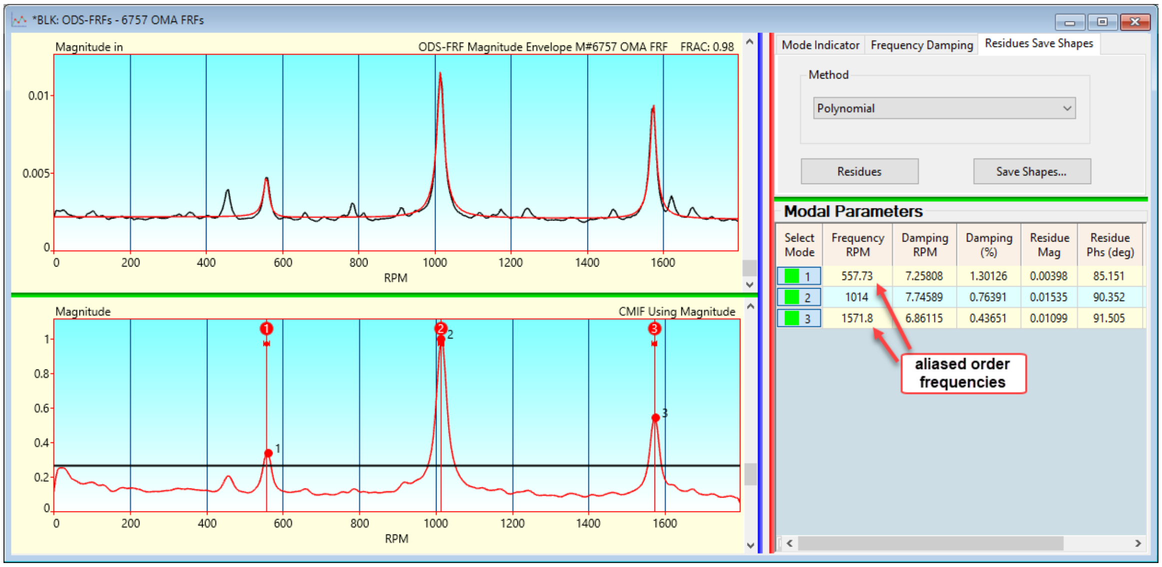

Select Mode	Frequency RPM	Damping RPM	Damping (%)	Residue Mag	Residue Phs (deg)
1	557.73	7.25808	1.30126	0.00398	85.151
2	1014	7.74589	0.76391	0.01535	90.352
3	1571.8	6.86115	0.43651	0.01099	91.505

Figure 6. Curve-fit of ODS-FRFs.

MODE SHAPES AT MONITORED POINTS

Although curve fitting was applied to all the **ODS-FRFs** calculated from the videos of the nine unbalance cases of the rotating machine, only the mode shape components are **five grid points** were labeled and archived in the machine database. These five points are labeled in Figure 7.

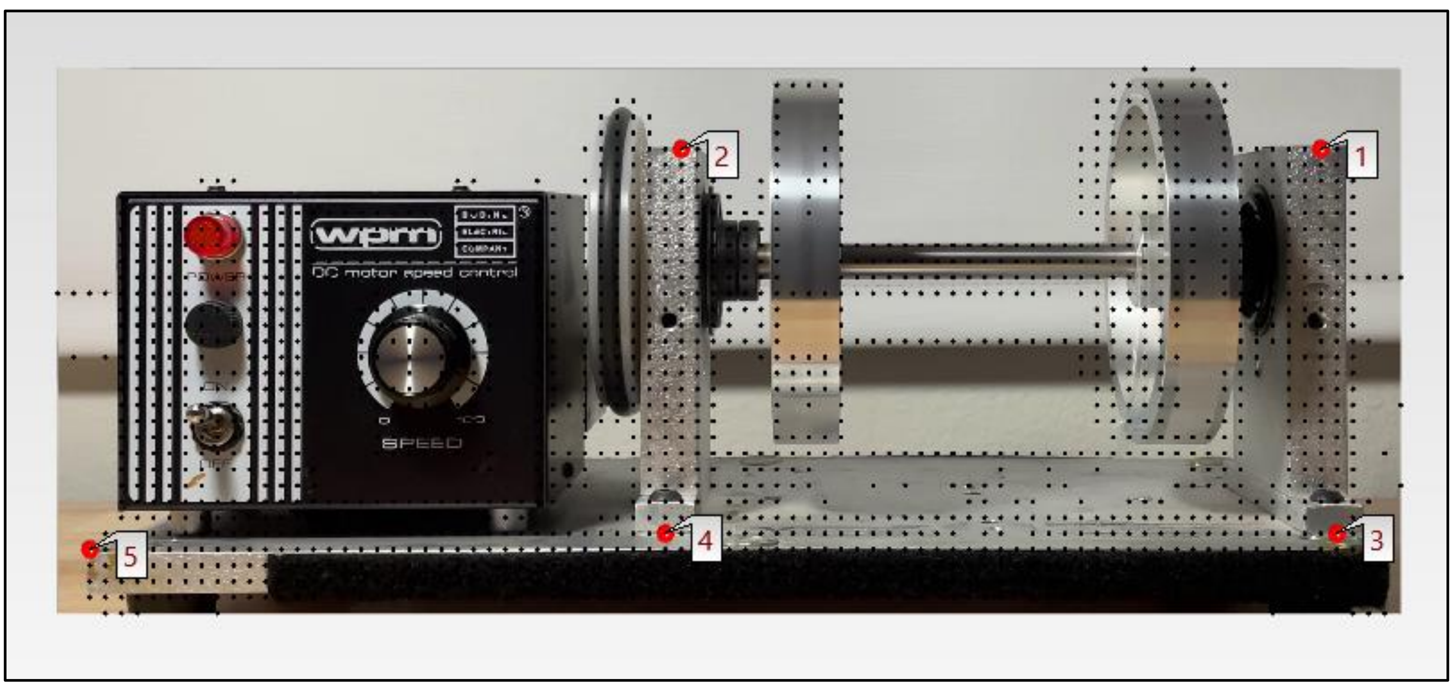

Figure 7. Point Grid Showing Monitored Points.

DAMPING REMOVAL

DeConvolution windowed is necessary before using an **FRF-based** curve fitter on a set of **ODS-FRFs**. But DeConvolution windowing ***adds a specific amount of damping*** to each **OMA** mode shape. Therefore, following curve fitting, when the **OMA** mode shapes are stored into a Shape Table in MEscope [9], the damping added by DeConvolution windowing is removed from them. This is shown in Figure 8.

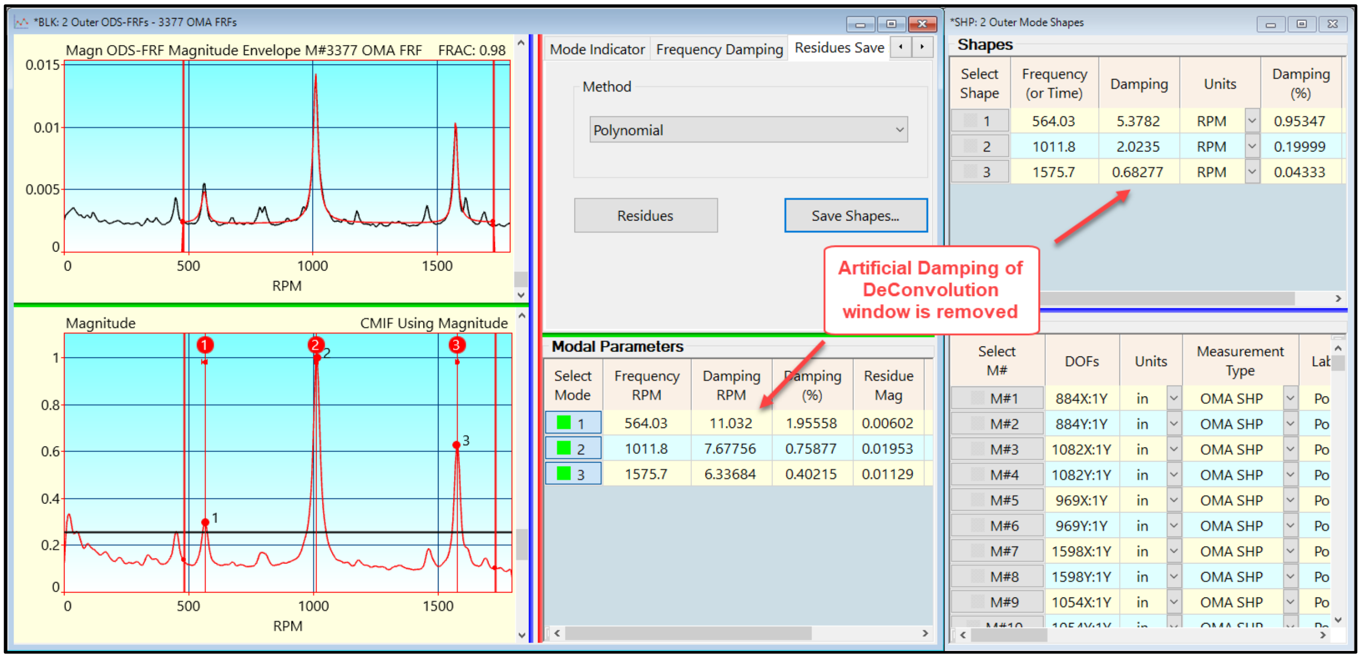

Figure 8. Damping is Removed when OMA Mode Shapes are Saved.

FaCTs™

FaCTs™ [4] is a database search algorithm used by MEscope [9]. **FaCTs** searches a database of ***labeled*** mode shapes, each **mode shape** associated with ***a particular machine fault***. When a new mode shape is saved into the archival database, **FaCTs** searches the database of ***labeled*** mode shapes and displays a bar chart of the ***ten closest matching* mode shapes** together with the mechanical fault associated with each ***labeled*** mode shape.

FaCTs™ uses an algorithm called the **Shape Difference Indicator (SDI)** [8]. **SDI** calculates a correlation coefficient between two complex-valued shape vectors. **FaCTs** finds the ***ten closest matching*** mode shapes in the archival database based on the **SDI** value between a ***current*** mode shape and each ***labeled*** mode shape in the database.

- **FaCTs** has values **between 0.0 and 1.0**
- **FaCTs** = **1.0 ➔** two mode shapes are ***identical***
- **FaCTs >= 0.9 ➔** two mode shapes are ***similar***
- **FaCTs** < **0.9 ➔** two mode shapes are ***different***

BASELINE CASE

When no unbalance screws were added to either rotor of the rotating machine in Figure 1, its mode shapes were labeled as the Baseline case. When the Baseline case is archived into the database, the **FaCTs** bar chart in Figure 9 clearly identifies it by its unique **OMA** mode shapes compared to the mode shapes of the other unbalance cases. Its **FaCTs** bars with all the other unbalance cases are ***much less than* 1.0**.

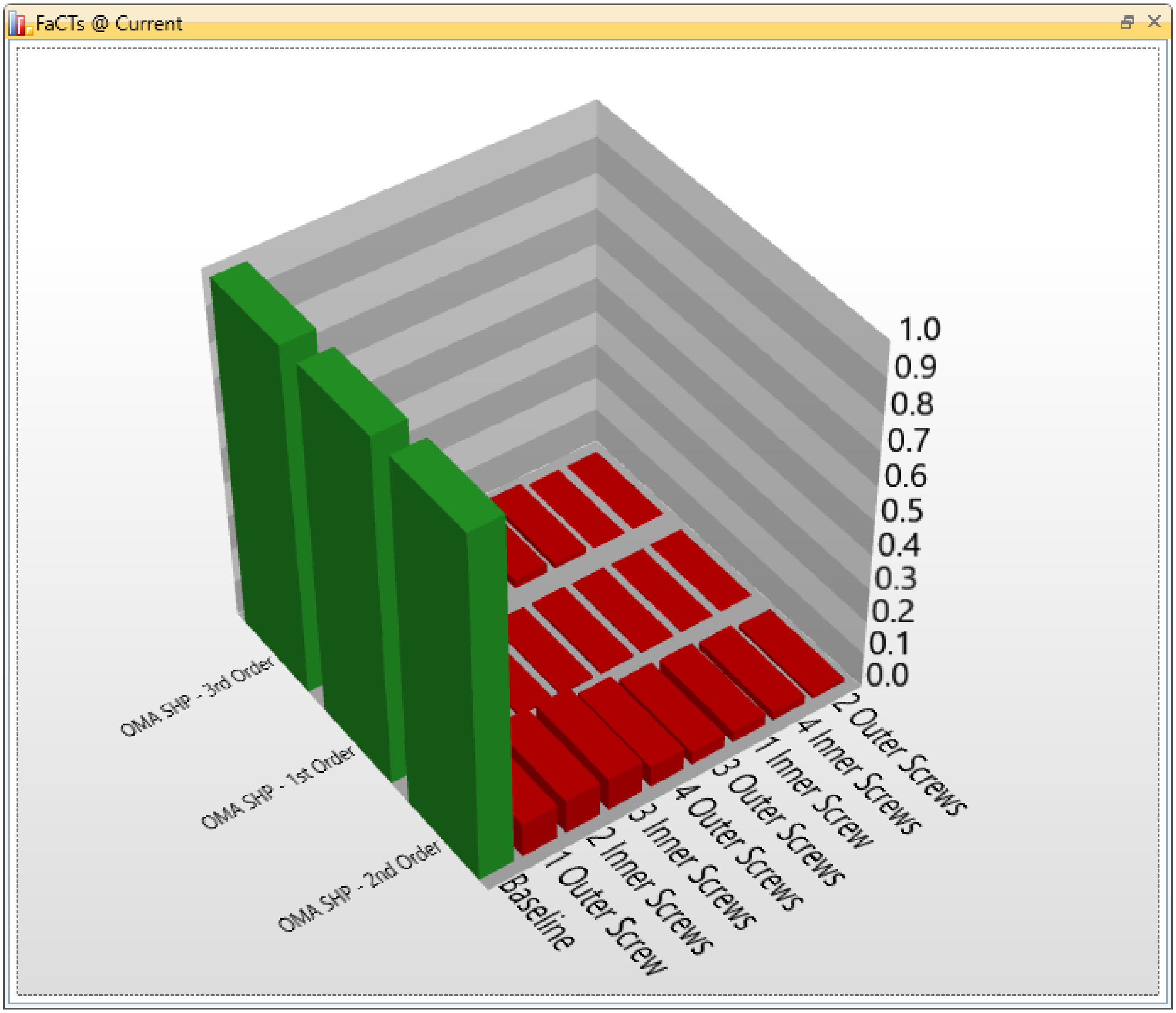

Figure 9. Baseline OMA Mode Shapes Versus Other Eight Unbalance Cases

Figures 10 through 18 show the **FaCTs** bar charts for the ***eight unbalance cases*** where screws were added to either the Inner or Outer rotor. Each unbalance case was ***uniquely identified*** by **FaCTs** because its corresponding **OMA** mode shapes were unique when compared to the **OMA** mode shapes of the other unbalance cases.

But ***there is one exception***. Unbalance cases with **2 Inner screws** and **3 Inners screws** have a **FaCTs** bar of **1.0**, indicating that the **OMA** mode shapes for these two cases ***are essentially the same***.

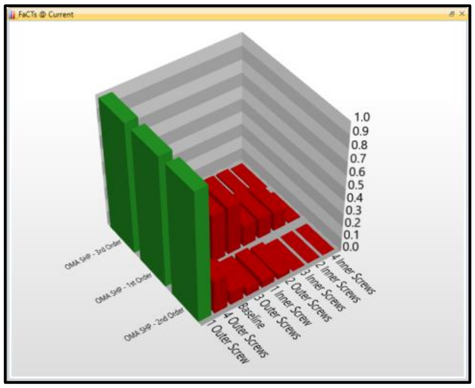

Figure 10. One Outer Screw

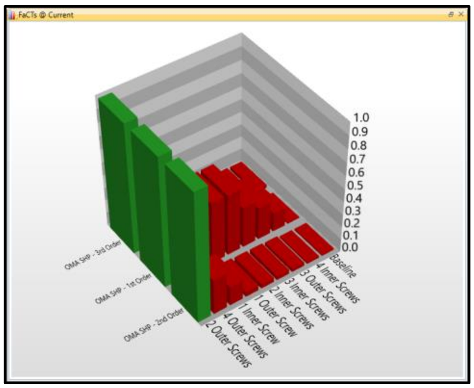

Figure 11. Two Outer Screws

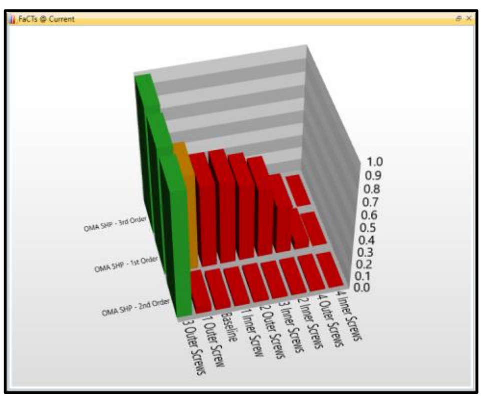

Figure 13. Three Outer Screws

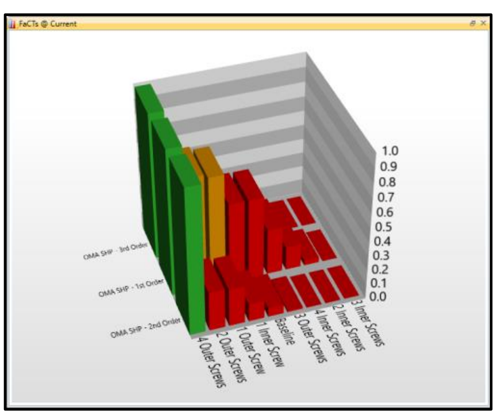

Figure 14. Four Outer Screws

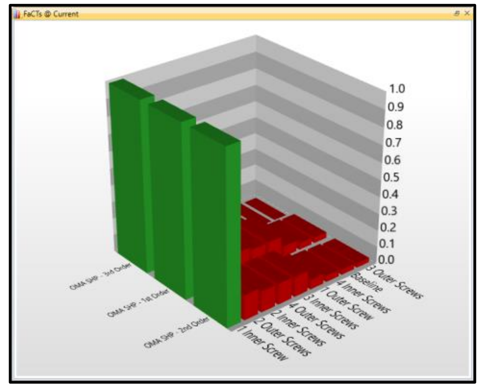

Figure 15. One InnerScrew

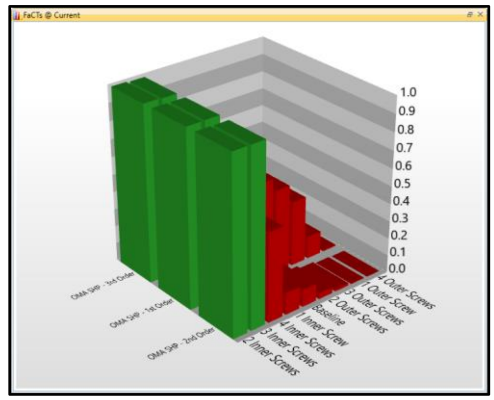

Figure 16. Two InnerScrews

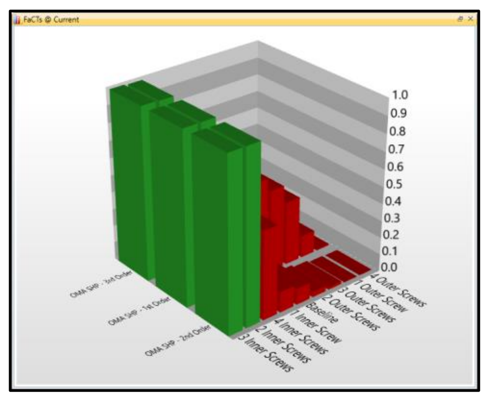

Figure 17. Three InnerScrews

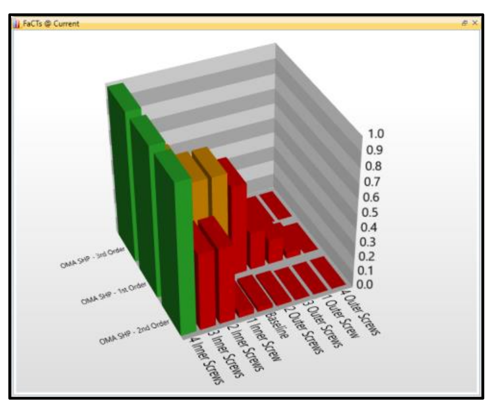

Figure 18. Four InnerScrews

CONCLUSIONS

Nine different unbalance cases were created on a rotating machine by adding screws to its ***Inner*** and ***Outer*** rotors. The first case with ***no screws added*** was labeled as the **Baseline** case. In each case, a **16 second** cell phone video was recorded, with the machine running at approximately **1000 RPM**.

Using MEscope [9], **TWFs** were extracted from each cell phone video and **ODS-FRFs** were calculated from the **TWFs** for each unbalance case. To reduce noise in the **ODS-FRFs**, five ***spectrum averages*** and ***overlap processing*** were used to calculate the **ODS-FRFs**. Then, the **ODS-FRFs** were curve fit using **FRF-based** curve fitting and the **OMA** mode shapes for the ***first three machine orders*** were labeled and stored in an archival database.

The **first order OMA** mode shape and the mode shapes of the **aliased second** and **third orders** were archived. Each set of three mode shapes was labeled with its ***corresponding unbalance case***.

Then, when the **OMA** mode shapes for each case were again calculated and stored into the archival database, **FaCTs** correctly identified each case by calculating its **SDI** value with each ***labeled*** set of **OMA** mode shapes in the database. This method of numerically comparing a ***current set*** of **OMA** mode shapes with sets of ***labeled*** **OMA** mode shapes uniquely identified each of the nine unbalance cases using only ***ten mode shape components*** from five points on the video point grid of the machine.

This low-cost approach using cell phone videos and **FaCTs** can be used by any plant maintenance department for monitoring the health of its rotating equipment and accurately identifying machine faults.

REFERENCES

[1] - S. Richardson, M. Richardson "Extracting 3D Mode Shapes from a Cell Phone Video" IMAC XLII, February 10-13, 2025, Orlando, FL.

[2] - B. Schwarz, S. Richardson, P. McHargue, M. Richardson "Using Modal Analysis and ODS Correlation to Identify Mechanical Faults in Rotating Machinery" IMAC XLII, January 29 - February 1, 2024, Orlando, TX.

[3] - D. Ambre, B. Schwarz, S. Richardson, M. Richardson, "Using Cell Phone Videos to Diagnose Machinery Faults" IMAC XLI, , Austin, TX, February 13-16, 2023.

[4] - B. Schwarz, S. Richardson, M. Richardson, "Using a Cell Phone Video and ODS Correlation to Diagnose Unbalance in Rotating Machinery" IMAC XLII, January 29 - February 1, 2024, Orlando, FL

[5] - M.H. Richardson, "Is It a Mode Shape or an Operating Deflection Shape?" Sound and Vibration magazine, March 1997.

[6] - B. Schwarz, M.H. Richardson, "Measurements Required for Displaying Operating Deflection Shapes" Proceedings of IMAC XXII, January 26, 2004

[7] - B. Schwarz, M.H. Richardson, "Introduction to Operating Deflection Shapes" CSI Reliability Week, Orlando, FL, October 1999

[8] - S. Richardson, J. Tyler, P. McHargue, M. Richardson "A New Measure of Shape Difference" IMAC XXXII February 3.6, 2014

[9] - MEscope™ is a trademark of Vibrant Technology, Inc. www.vibetech.com